Electrochemical Studies of Niobocene–Ketene Complexes: Redox-Induced Ketene Fragmentation Reactions

Anushuyadevi Savaranamuthu,[1a] Alice E. Bruce,*[,1a] Mitchell R. M. Bruce,*[,1a] Maria C. Fermin,[1b] Azzam S. Hneihen,[1b] and Joseph W. Bruno*[,1b]

Departments of Chemistry, University of Maine, Orono, Maine 04469, and Wesleyan University, Middletown, Connecticut 06459

Received November 25, 1991

The 18-electron ketene complexes *exo*-$(C_5H_4SiMe_3)_2Nb(Cl)(\eta^2\text{-}C,O\text{-}OCCR_2)$ undergo facile 1-electron reduction to the paramagnetic metallaenolate complexes $[(C_5H_4SiMe_3)_2Nb(Cl)(OCCR_2)]^-$. This process has been studied by cyclic voltammetry, electrolysis, and infrared spectroelectrochemistry, which indicate that the ketene complexes undergo a structural isomerization upon reduction. In addition, the metallaenolates have been studied by ESR spectroscopy and are found to have anomalously low ^{93}Nb hyperfine splittings; this has been attributed to the delocalization of unpaired spin density onto the enolate ligand, which suggests that the structural reorganization of the reduced complex involves rotation of the enolate ligand to facilitate this resonance delocalization. Infrared spectroelectrochemical studies also provide evidence as to the ultimate fate of the metallaenolate. These indicate that the anions undergo a slow and reversible loss of chloride and that the resulting coordinatively-unsaturated compounds undergo a subsequent ketene fragmentation; the product generated in this way is observed to contain a carbonyl ligand and is identified as an alkylidene–carbonyl complex. Upon subsequent reoxidation, some of the starting niobium–ketene complex is regenerated, and the overall process can be described as a redox-induced ketene cleavage–formation sequence. Finally, in the presence of added acids (Lewis or Brønsted), the electrochemistry goes via a two-electron sequence to give either niobocene alkyl–carbonyl or ketene–hydride complexes.

Introduction

There are now numerous examples in which organometallic compounds with π-complexed ligands undergo substantial structural isomerization upon reduction.[2] This is typically a consequence of the fact that reduction generates a 19-electron configuration, such that the ligand slips to reduce the electron density at the metal center. We have been pursuing the chemistry of a class of early-transition-metal–ketene complexes of general formula $Cp'_2Nb(X)(ketene)$ ($Cp' = \eta^5\text{-}C_5H_4SiMe_3$);[3] these are 18-electron compounds in which the ketene ligand is bound via complexation of the C=O bond. We became interested in the prospect of reducing these complexes with the expectation that the added electron could end up localized in an orbital which is largely ketene-π^* in character. This would convert the 18-electron complex into (nominally) a 19-electron metallaenolate complex, and this might be expected to induce a geometrical rearrangement. Metallaenolates are themselves of considerable interest since they constitute reactive nucleophiles which are readily capable of condensation and trapping reactions;[4] these reactions can be rendered stereoselective with the proper choice of ancillary ligand set.

Another rationale for the current study is based on the suggestion that ketenes can function as intermediates in metal-catalyzed carbon monoxide homologation processes.[5] They are believed to arise from the coupling of CO and methylene moieties on the catalyst surface (eq 1), and this

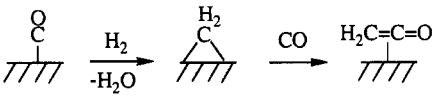

(1)

process has been amply modeled in homogeneous systems.[6] In addition, it has recently been suggested that uncomplexed ketenes are involved in the primary carbon–carbon bond-forming reaction in the zeolitic conversion of methanol to hydrocarbons.[7] Our electrochemical and infrared spectroelectrochemical studies on niobocene–ketene complexes (reported herein) provide evidence for structural isomerization upon one-electron reduction, followed by a slower redox-induced ketene cleavage and recombination sequence; we have also observed the operation of a Lewis acid-induced two-electron reduction pathway. In addition, we will present ESR data relating to the structure of a proposed metallaenolate intermediate derived from reduction of the ketene complexes.[8]

Experimental Section

General Considerations. All manipulations were carried out under an atmosphere of nitrogen which was purified by passage through a column of Linde 4A molecular sieves and activated BTS catalyst. Solutions were handled using standard Schlenk methods, and solids were transferred in a Vacuum Atmospheres Corp.

(1) (a) University of Maine. (b) Wesleyan University.

(2) (a) Paw Blaha, J.; Wrighton, M. S. *J. Am. Chem. Soc.* **1985**, *107*, 2694–2702. (b) Monkeberg, S.; van Raaij, E.; Kiesele, H.; Brintzinger, H.-H. *J. Organomet. Chem.* **1989**, *365*, 285. (c) Tyler, D. R.; Philbin, C.; Fei, M. In *Paramagnetic Organometallic Species in Activation/Selectivity, Catalysis*; Chanon, M., Julliard, M., Poite, J. C., Eds.; Kluwer Academic: Dordrecht, 1989. (d) Geiger, W. E. *Prog. Inorg. Chem.* **1985**, *33*, 275–352 and references therein.

(3) (a) Halfon, S. E.; Fermin, M. C.; Bruno, J. W. *J. Am. Chem. Soc.* **1989**, *111*, 5490–5491. (b) Bruno, J. W.; Fermin, M. C.; Halfon, S. E.; Schulte, G. K. *J. Am. Chem. Soc.* **1989**, *111*, 8738–8740. (c) Fermin, M. C.; Hneihen, A. S.; Bruno, J. W.; Schulte, G. K. Manuscript in preparation.

(4) Leading references: (a) Liebeskind, L. S.; Walker, M. E.; Fengl, R. W. *J. Am. Chem. Soc.* **1986**, *108*, 6328–6343. (b) Rusik, C. A.; Collins, M. A.; Gamble, A. S.; Tonker, T. L.; Templeton, J. L. *J. Am. Chem. Soc.* **1989**, *111*, 2550–2561. (c) Davies, S. G. *Pure Appl. Chem.* **1988**, *60*, 13–20. (d) Berno, P.; Floriani, C.; Chiesi-Villa, A.; Guastini, C. *Organometallics* **1990**, *9*, 1995–1997.

(5) (a) Anderson, R. B. *The Fischer–Tropsch Synthesis*; Academic Press: Orlando, FL, 1984; Chapter 5 and references therein. (b) Keim, W. *J. Organomet. Chem.* **1989**, *372*, 15–23. (c) Dry, M. E. *J. Organomet. Chem.* **1989**, *372*, 117–127.

(6) (a) Herrmann, W. A.; Plank, J. *Angew. Chem., Int. Ed. Engl.* **1978**, *17*, 525–526. (b) Barger, P. T.; Santarsiero, B. D.; Armantrout, J.; Bercaw, J. E. *J. Am. Chem. Soc.* **1984**, *106*, 5178–5186. (c) Miyashita, A.; Shitara, H.; Nohira, H. *Organometallics* **1985**, *4*, 1463–1464. (d) Geoffroy, G. L.; Bassner, S. L. *Adv. Organomet. Chem.* **1988**, *28*, 1–83.

(7) Jackson, J. E.; Bertsch, F. M. *J. Am. Chem. Soc.* **1990**, *112*, 9085–9092.

(8) Portions of this work were presented at the "Organometallic Electrochemistry" symposium held at the 200th National Meeting of the American Chemical Society, Washington, D.C., Aug 27–31, 1990.

0276-7333/92/2311-2190$03.00/0

glovebox. Solvents toluene, hexane, and tetrahydrofuran were purchased from J.T. Baker and distilled from sodium benzophenone ketyl under nitrogen. The preparations of the niobium-ketene complexes $Cp'_2Nb(Cl)(OCCRR')$ (1, R = Et, R' = Ph; 2, R = R' = Ph; 3, R = R' = Me) and $Cp'_2Nb(H)(OCCRR')$ (9, R = Et, R' = Ph; 10, R = R' = Ph; 11, R = R' = Me) have been described elsewhere.[3] Electrolytes tetra-*n*-butylammonium tetrafluoroborate and tetra-*n*-butylammonium chloride (Aldrich) were subjected to prolonged evacuation and thereafter handled only under nitrogen. The supporting electrolyte tetra-*n*-butylammonium hexafluorophosphate (TBAH) was prepared by metathesis of tetra-*n*-butylammonium bromide (Aldrich) and HPF_6 (Aldrich) in H_2O, purified by reprecipitation from CH_2Cl_2/ether, and dried in vacuo at 80 °C for 24 h.

Proton NMR spectra were obtained on a Varian XL-400 FT-NMR instrument and X-band ESR spectra were obtained on a Bruker ESP 300 spectrometer using 4-mm quartz tubes; *g* values are uncorrected. Routine IR spectra were determined using 0.05-mm path length liquid cells on a Perkin-Elmer Model 1600 FT-IR spectrometer. GC–mass spectra were obtained on a Hewlett-Packard GC (5890)–MS (5988A) system using a 50-ft capillary column. Voltammograms were measured using a Princeton Applied Research EG&G VersaStat potentiostat and three-electrode system consisting of a platinum button working electrode, platinum wire counter electrode, and $Ag/AgNO_3$ reference electrode.

Constant Current Electrolysis. Constant current electrolyses were carried out with a Kepco power supply and an undivided cell consisting of stainless steel mesh cathode and magnesium rod sacrificial anode. The cell was a 25-mm-i.d. test tube with a septum cap, through which electrode wires were passed; it was configured with a cylindrical cathode screen ringing the inside of the tube and the magnesium rod suspended in the center of the cylindrical cathode.

Constant Potential Electrolysis. Constant potential electrolyses were carried out with a Princeton Applied Research EG&G Model 273 potentiostat/galvanostat. A three-compartment cell designed for handling air-sensitive materials was used for all constant potential electrolysis experiments.[9] The reference electrode was a saturated potassium chloride calomel electrode (SCE) brought into the main compartment via a lugin capillary. The main compartment contained a cylindrical Pt mesh electrode and a Teflon stir bar centered within the Pt mesh. The auxiliary Pt mesh electrode was separated from the main compartment by a fine porosity glass frit.

The electrolyte solution, 0.5 M TBAH/THF, was introduced into the cell and was degassed with nitrogen for a minimum of 10 min with stirring. For electrolysis experiments with added chloride, the electrolyte solution contained a mixture of 0.4 M TBAH/THF and 0.1 M (TBA)Cl. The solution was potentiostated at ≤−2.1 V vs SCE, and after the current had reached a steady state (typically within 5–10 min), the background current (i_{bkg}) was measured. The complex under investigation was then added and the degassing process repeated. The internal coulometer of the PAR 273 was reset, and the same potential used to determine the background current was then applied. Electrolysis was assumed to be complete when $i_{exp} \cong i_{bkg}$. The total number of electron equivalences, *n*, passed during the constant potential electrolysis experiment was calculated by assuming that the process contributing to the background current continued during the electrolysis experiment. Thus, the total number of coulombs representing the background process (Q_{bkg}) was subtracted from the total number of coulombs passed during the experiment (Q_{total}). The following equation was used to determine *n*:

$$n = \frac{Q_{total} - Q_{bkg}}{F(\text{mol})}$$

where *F* is the Faraday constant and mol is the number of moles of substrate added. Constant potential electrolyses of ferrocene at +1.5 V vs SCE, used to calibrate the cell, gave an average *n* value of 0.93 (expected *n* = 1.0).

(9) Bolinger, C. H.; Story, N.; Sullivan, B. P.; Meyer, T. J. *Inorg. Chem.* **1988**, *27*, 4582.

Infrared Spectroelectrochemical Studies. FT-IR spectroelectrochemical studies were carried out using a transmission spectroelectrochemical cell consisting of a platinum screen working electrode (52 mesh), platinum wire counter electrode, and silver wire pseudoreference sandwiched between sodium chloride plates. The cell design has been described previously.[10] The cell was placed in a Midac FT-IR spectrophotometer (Model 101025) contained within a glovebox. The spectrophotometer was interfaced externally to a Zenith computer (Model ZDE-1217-130) and was controlled using Spectra Calc software (Galactic Industries). The spectroelectrochemical cell was connected to the EG&G Applied Research 273 potentiostat, and the entire electrochemical procedure was carried out inside the glovebox. In a typical experiment, the FT-IR cell was filled with electrolyte solution (TBAH, 0.7 M in THF) and a background spectrum was recorded; this was subsequently subtracted from all spectra recorded for the complex solution. The cell was then filled with a solution containing the niobocene–ketene complex (5–10 mM) and an initial spectrum recorded. A reduction experiment was begun by setting the spectroelectrochemical working electrode to ca. −3 V vs the silver pseudoreference, and the changes in the infrared region were monitored by obtaining spectra at frequent intervals (every 30–120 s) using four transients at 4-cm^{-1} resolution.

$Cp'_2Nb(CO)(CHEtPh)$ (6). In a typical synthetic procedure, the undivided cell was equipped as described above for constant current electrolysis (sacrificial Mg anode and stainless steel mesh cathode) and charged with 250 mg (0.46 mmol) of $Cp'_2Nb(Cl)(OCCEtPh)$. This was dissolved in 10 mL of a THF solution which was 0.45 M in $NBu_4^+BF_4^-$. The resulting yellow solution was electrolyzed at a current of 100 mA for ca. 15 min (0.92 mfaraday), during which time the solution turned brown; the extent of reaction was monitored by removing aliquots for infrared spectroscopy. The resulting solution was removed from the cell via syringe and the solvent removed in vacuo. The residue was extracted with hexane and the hexane removed to leave a brown oily solid. Attempts to crystallize this highly soluble material were unsuccessful. IR (THF solution): 1899 cm^{-1}. ^1H NMR (C_6D_6): 8.12 (d), 7.81 (d), 6.91 (m), 5.05, 4.99, 4.65, 4.61, 4.45, 4.10, 3.90 (all broad singlets), 2.70 (m), 1.79 (m), 1.01 (t), 0.08 (s), and 0.01 (s). A similar procedure was utilized to prepare $Cp'_2Nb(CO)(CHPh_2)$ (7) and $Cp'_2Nb(CO)(CHMe_2)$ (8). Spectral data for 7. IR (THF): 1907 cm^{-1}. ^1H NMR (C_6D_6): 8.15 (d), 7.80 (d), 7.35 (m), 6.88 (m), 5.50, 5.23, 4.70, 4.20 (all broad singlets), 2.45 (s), and 0.18 (s). Spectral data for 8. IR (THF): 1890 cm^{-1}. ^1H NMR (C_6D_6): 5.20, 4.73, 4.50, 4.40 (all broad singlets), 2.4 (septet), 1.45 (d), and 0.15 (s).

Results

Voltammetric Studies. The cyclic voltammetry done in this work was carried out in THF with reference to a $Ag/AgNO_3$ reference electrode, so the observed waves are shifted approximately 0.35 V negative (e.g., in the cathodic direction) relative to processes carried out with a SHE reference.[11] Typical voltammograms for $Cp'_2Nb(Cl)(OCCEtPh)$ (1) and $Cp'_2Nb(Cl)(OCCPh_2)$ (2) are shown in Figure 1. For compound 1, the initial cathodic sweep results in a broad reduction wave at −2.10 V. On the return sweep, one observes an anodic wave (−1.85 V) which is well separated from the cathodic wave. If the same potential range is immediately swept again, one observes a new reduction wave at ca. −1.95 V, as well as the previously observed oxidation wave at −1.85 V. Clearly there was no evidence for the former on the first sweep, indicating that the species responsible for it was formed as a result of the redox chemistry. The cathodic and anodic waves observed on the second sweep are separated by ca. 100 mV, a separation similar to that observed for Cp_2Fe/Cp_2Fe^+ under

(10) Saravanamuthu, A.; Bruce, A. E.; Bruce, M. R. M. *Vib. Spectrosc.* **1991**, *2*, 101–106.

(11) (a) Fry, A. J.; Britton, W. E. In *Laboratory Techniques in Electroanalytical Chemistry*; Kissinger, P. T., Heineman, W. R., Eds.; Marcel Dekker: New York, 1984; Chapter 13. (b) Kadish, K. M.; Ding, J. Q.; Malinski, T. *Anal. Chem.* **1984**, *56*, 1741–1744.

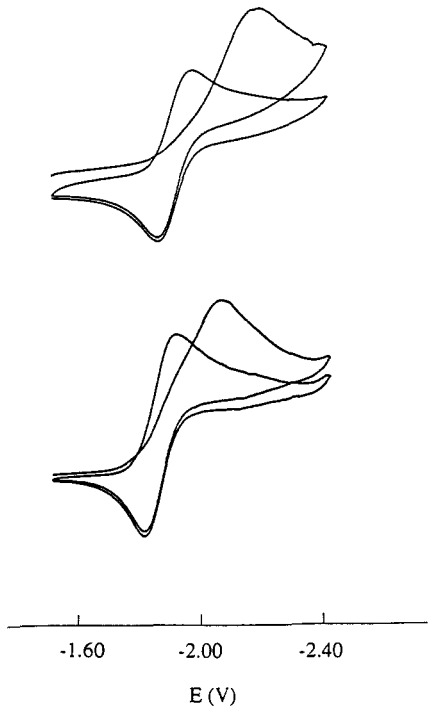

Figure 1. (a, top) Cathodic voltammogram for **1** in 0.8 M $NBu_4^+BF_4^-$ TNF using a platinum button working electrode, scan rate 50 mV/s. (b, bottom) Corresponding voltammogram for **2**. Potentials are vs $Ag/AgNO_3$.

Table I. Solution ESR Data for Radical Anions[a]

compound	⟨g⟩	⟨a⟩, G
$[Cp'_2Nb(Cl)(OCCEtPh)]^-$ (4^-)	2.000	16
$[Cp'_2Nb(Cl)(OCCPh_2)]^-$ (5^-)	1.997	16

[a] Prepared via electrolysis of **1** or **2** in THF solution containing 0.6 M $NBu_4^+BF_4^-$; solutions were diluted with an equal volume of toluene to avoid excessive microwave absorption by solvent.

comparable experimental conditions (THF solution, 0.8 M $NBu_4^+BF_4^-$, sweep rates 25–100 mV/s; $E_{1/2}$ = 0.074 V vs $Ag/AgNO_3$ for Fc/Fc^+); as such, these peaks are proposed to result from a reversible redox couple. Compound **2** exhibits qualitatively similar behavior (Figure 1b), although the peak potentials are shifted appreciably in the anodic direction relative to those of **1**. The voltammetric behavior is consistent with a mechanism in which electron-transfer events are coupled to thermal processes, i.e., an EC mechanism.[2d]

ESR Spectra. To gather more information regarding the nature of the reduction processes, we carried out the electrochemical reduction of $Cp'_2Nb(Cl)$(ketene) compounds **1** and **2** (eq 2) at low temperature (0 °C, divided

$$Cp'_2Nb(Cl)(OCCRR') \xrightarrow[THF]{e^-} [Cp'_2Nb(Cl)(OCCRR')]^{-\bullet} \quad \begin{matrix} 4^-\text{: R = Et, R' = Ph} \\ 5^-\text{: R = R' = Ph} \end{matrix} \qquad (2)$$

cell), transferred the cold solutions to quartz ESR tubes under inert atmosphere, and obtained room-temperature spectra immediately. Under these conditions, we observe a 10-line spectrum for anions 4^- and 5^- (as the NBu_4^+ salt); g values and isotropic hyperfine constants $\langle a \rangle$ are given in Table I, and the spectrum for 4^- is shown in Figure 2. Related studies on **3** were unsuccessful as the resulting radical anion is prone to a subsequent reaction, the nature of which is not yet clear. It is apparent that the 10 lines in the spectrum of 4^- (Figure 2a) exhibit variations in line width, such that the outer lines are considerably broadened

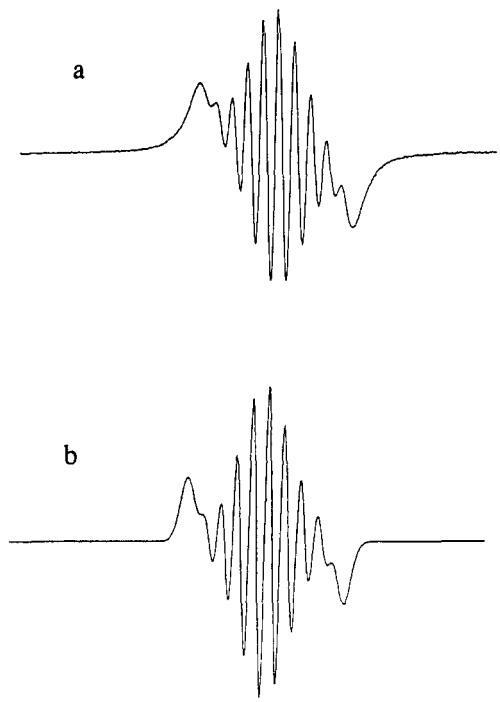

Figure 2. (a) X-band ESR spectrum of 4^- in 3:1 touene/THF. (b) Simulated spectrum (see text).

relative to the inner lines; the spectrum of 5^- is similar in this regard. This phenomenon is not altogether unusual and can be expected for radicals with a large rotational correlation time. Fraenkel has discussed the theory of ESR line widths,[12] and for the systems at hand, we may identify three expected contributions to the observed line widths (Γ); these are indicated in eq 3. There is an intrinsic line

$$\Gamma = A + \sum_i B_i M_i + \sum_i C_i M_i^2 \qquad (3)$$

width A that encompasses the various broadening mechanisms contributing equally to all spectral lines. This may be supplemented by the B- and C-term contributions, which are summed over all i identical coupled nuclei. The former is related to the product of the anisotropies in the g and hyperfine tensor and results in broadening of the spectral lines derived from higher nuclear spin terms (M_I); the current spectra show little obvious evidence of this contribution. The C-term broadening is derived from the hyperfine anisotropy alone and depends on M_I^2; as such, it is relatively unimportant for center lines and contributes to increasing widths for the outermost lines of a multiplet signal. To verify that this was the only cause of the observed line broadening, we carried out the spectral simulation shown in Figure 2b.[13] This simulated spectrum was obtained by using one $I = {}^9/_2$ nucleus, an intrinsic line width A = 5.7 G, a C contribution of 2.0 G, and an isotropic hyperfine splitting constant $\langle a \rangle$ = 16 G; the close agreement between experimental and simulated spectra suggests that one chemical species is giving rise to the spectrum. Low-temperature studies uncovered no evidence for an equilibration process, and frozen solution spectra exhibited

(12) (a) Fraenkel, G. K. *J. Chem. Phys.* **1967**, *71*, 139–171. (b) See also: Wertz, J. E.; Bolton, J. R. *Electron Spin Resonance*; Chapman and Hall: New York, 1986; Chapter 9. (c) Symons, M. C. R. *Chemical and Biochemical Aspects of Electron-Spin Resonance Spectroscopy*; John Wiley & Sons: New York, 1978; Chapter 5.

(13) The ESR simulation was done with the program QPOW. (a) Nilges, M. J. Ph.D. Thesis, University of Illinois, Urbana, 1979. (b) Belford, R. L.; Nilges, M. J. *Computer Simulation of Powder Spectra*, EPR Symposium, 21st Rocky Mountain Conference, Denver, CO, Aug 1979. (c) Maurice, A. M. Ph.D. Thesis, University of Illinois, Urbana, 1980.

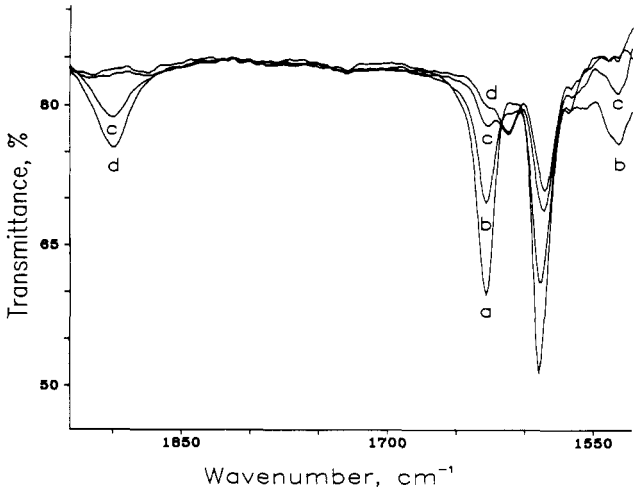

Figure 3. Infrared spectroelectrochemical data for reduction of 1; (a) time = 0, (b) 8, (c) 14, and (d) 20 min. Applied potential was removed at time = 10 min.

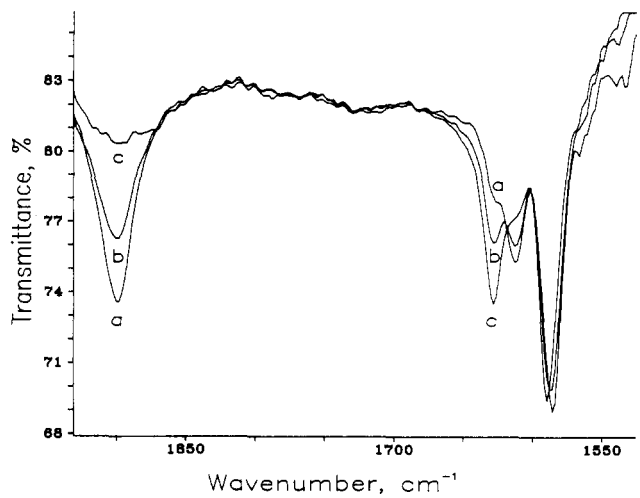

Figure 4. Infrared spectroelectrochemical data for oxidation. First spectrum corresponds to spectrum d in Figure 4 (rescaled); subsequent spectra were taken after the application of oxidizing potential.

the expected large hyperfine anisotropies.

Infrared Spectroelectrochemical Studies. To gather additional information on the solution behavior of the reduced ketene complexes, we turned to in situ infrared spectroscopy. The complexed ketenes exhibit infrared bands at approximately 1620 cm^{-1} due to C=C-based stretching vibrations. As such, a reduction that adds electron density to ketene-based antibonding orbitals (presumably C–C π^*) should give rise to a new band at lower energy. Figures 3 and 4 illustrate the results of these studies. The first spectrum in Figure 3 shows infrared absorption bands at 1623 and 1585 cm^{-1} for the starting ketene complex (1) in THF solution (also containing 0.7 M TBAH). After this spectrum was recorded, the cell potential was stepped to ca. −3.0 V vs the silver wire pseudoreference[14] and spectra were recorded at regular intervals. In the second spectrum (Figure 3b), it is apparent that the 1623-cm^{-1} band has diminished in favor of a new broad band at 1530 cm^{-1}. The electrolysis is continued until this process is largely complete, *at which time the applied potential is removed.* As the third spectrum (Figure 3c) indicates, there is a slow thermal reaction which depletes the 1530-cm^{-1} band in favor of a stronger band at 1901 cm^{-1}, and this process is largely complete in the fourth spectrum (Figure 3d); also evident is a weak band at ca. 1610 cm^{-1}.

If an oxidizing potential of +0.4 V is now applied (Figure 4), the bands at 1901 and 1610 cm^{-1} are replaced by bands due to starting material; note that separate control experiments verified that the starting ketene complexes are not oxidized at +0.4 V. In contrast, if no oxidizing potential is applied, the strong band observed in the IR at ca. 1901 cm^{-1} slowly gives way to a broader and weaker band at 1915–1920 cm^{-1} over a period of 15–25 min. The exact position of the higher energy band is somewhat obscured by the strong band at ca. 1901 cm^{-1} as well as by the THF overtone band which occurs in this region. We note that if the solution is reoxidized at +0.5 V *before* the band at 1901 cm^{-1} appears, some of the starting ketene complex is regenerated.

Infrared Spectroelectrochemical Studies with Added Chloride Salt. The FT-IR spectroelectrochemical studies described above were repeated in the presence of a 10-fold excess of chloride, added as $NBu_4^+Cl^-$ (0.1 M). The reduction of the ketene complex initially proceeds as in the experiments without added chloride to form the species responsible for the band at 1530 cm^{-1}. However, when the applied potential is removed, the rate of thermal conversion of this species to that responsible for the 1901-cm^{-1} band is considerably diminished. For example, in the presence of added chloride, this process is only 10–20% complete after 20 min. In contrast, without added chloride, this process is largely complete within 20 min.

Constant Potential Electrolyses. Experimental n values of 1.02, 1.05, and 1.07 were obtained for reduction of 1 at ≤−2.1 V vs SCE. Infrared spectra taken upon completion of electrolysis show that the bands for the starting ketene complex have disappeared and have been replaced by the broad band at ca. 1901 cm^{-1}. In contrast, IR spectra taken upon completion of electrolysis experiments with added chloride reveal the presence of the 1530-cm^{-1} band as well as the band at 1901 cm^{-1}. The value of n does not change with added chloride.

Preparative Studies. In an attempt to carry out redox chemistry on a preparative scale, the ketene complexes were reduced in an undivided cell in THF solution. In view of the low conductivity of this solvent, initial reactions were run with high electrolyte concentrations and with a sacrificial magnesium anode. The reaction was monitored by infrared spectroscopy, and spectra are shown in Figure 5 for a reaction run on 1 under conditions of constant current. Again, the presence of the ketene complex is indicated in the first spectrum, but spectra taken during electrolysis show depletion of the band at 1623 cm^{-1}. In addition, a new band at 1899 cm^{-1} is seen, and in this reaction it appears immediately after the onset of electrolysis. The preparation of the new compound (6) is a clean process, and we can use infrared absorption intensities to monitor the course of the reaction under constant current electrolysis; this should give rise to a linear change in concentration as a function of electrolysis time. Figure 6 presents a plot of starting material concentration (from the intensity of the 1623-cm^{-1} band), product concentration (from the intensity of the 1899-cm^{-1} band), and the sum of the two. As is clear, the latter is virtually horizontal, indicating that the total amount of organoniobium in solution is constant; in other words, this conversion is clean and little or no niobium compound is being siphoned into a nonproductive avenue.

(14) Due to the iR drop in the FT-IR spectroelectrochemical cell, an overpotential must be applied to observe prompt electrochemistry. Experiments performed at −2.5 V vs Ag wire show qualitatively identical results, albeit at slower rates.

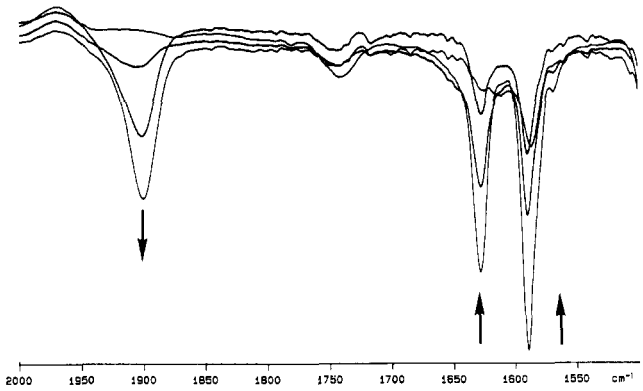

Figure 5. Infrared data for the constant-current (25-mA) reduction of 1 (10 mM) in 0.6 M $NBu_4^+BF_4^-$/THF in an undivided cell containing a sacrificial magnesium anode. Spectra correspond to electrolysis times 0, 210, 420, and 720 s.

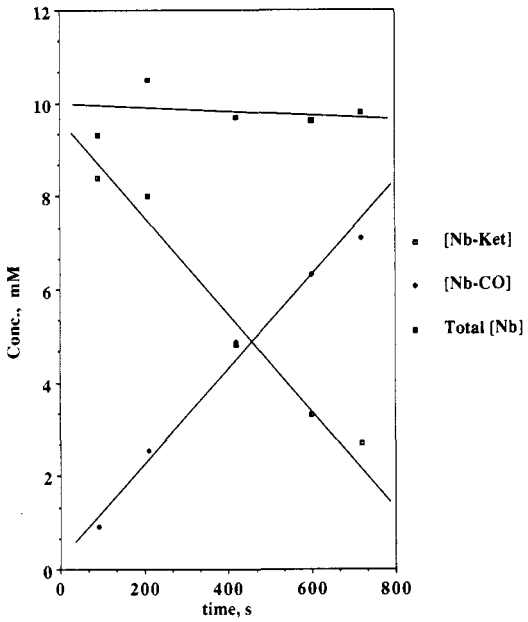

Figure 6. Concentration profiles for the constant-current electrolysis of 1 in THF solution (undivided cell, magnesium anode).

Coulometric studies indicate that the production of **6** is a two-electron process, suggesting a Nb(III) formulation (eq 4). We have isolated the Nb(III) compound as an

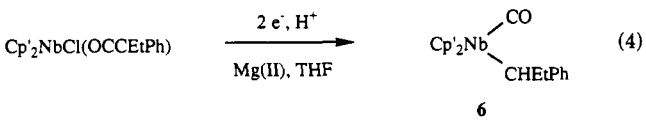

(4)

6

air-sensitive brown oily solid; it can be extracted from electrolyte but is often contaminated with small amounts of the known compound $Cp'_2Nb(Cl)(CO)$.[15] For **6** we observe NMR data (see Experimental Section) indicating a lack of mirror symmetry, since there are eight resonances for the inequivalent Cp′ ligands. We also observe signals consistent with the presence of the CHEtPh ligand, which is thus presumably responsible for the lack of symmetry. As an alternate confirmation of this, we hydrolyzed some of the compound and analyzed the resulting organic product mixture via GC–MS; this indicated the presence of Cp′H (*m/e* 138) and 1-phenylpropane (*m/e* 120), and the identity of the latter was confirmed by comparison to an authentic sample. We also note that the analogues $Cp'_2Nb(CO)(CHPh_2)$ (**7**) and $Cp'_2Nb(CO)(CHMe_2)$ (**8**) derived from complexes of symmetrically-substituted ketenes (e.g., **2** and **3**) have been identified similarly, and their ^1H NMR spectra contain only four resonances for the equivalent Cp′ ligands.

Discussion

One-Electron Redox Chemistry. Cyclic voltammograms indicate that a new redox-active complex forms upon reduction of $Cp'_2Nb(Cl)$(ketene) complexes (Figure 1), and constant potential electrolysis of 1 indicates that reduction is a one-electron process. Spectroelectrochemical experiments demonstrate that the reduction produces a complex with a broad infrared band at 1530 cm^{-1} which is stable over a period of several minutes. Assignment of this complex (4^-) as a metallaenolate is consistent with literature reports of the infrared characteristics of organic ketone enolates, which are found to exhibit bands in a similar region of the spectrum.[16] In addition, this assignment is consistent with the ESR data discussed next.

ESR Data. The ketene complexes discussed herein are most reasonably formulated as Nb(V) compounds if one considers binding to involve considerable back-bonding into the ketene LUMO. Single-electron reduction would be expected to generate what is formally a Nb(IV) compound, and the d^1-electron configuration makes these particularly amenable to study via ESR spectroscopy. Indeed, a number of niobocene derivatives (Cp_2NbX_2) have been studied,[17] and certain characteristics have been noted. First, these compounds exhibit 10-line ESR signals due to hyperfine splitting by the ^{93}Nb nucleus (100% natural abundance, $I = {}^9/_2$), and g values are close to the free-electron value (ca. 2.0). In addition, hyperfine splittings are typically on the order of 80–120 G for niobocene compounds with halide or alkyl coligands, while some hydride and sulfide derivatives exhibit lower $\langle a \rangle$ values (25–46 G).[18]

Clearly, our compounds 4^- and 5^- constitute exceptions to the foregoing generalizations since both exhibit $\langle a \rangle$ values of ca. 16 G. The simplest explanation for this is a diminished unpaired spin density at the ^{93}Nb center, consistent with delocalization of unpaired spin density onto the ligand set. Since other niobocene halides fail to exhibit this behavior, it is logical to implicate the ketene ligand in the process. Further, we propose that the radical ion still has chloride in the coordination sphere since spectra were collected immediately following electrochemical reduction of the niobocene–ketene complexes and because the FT-IR spectroelectrochemical studies show that 4^- loses chloride over a span of minutes at room temperature. Thus, the radical anion produced upon reduction is most reasonably represented by the two canonical structures shown below (metallaallylic delocalization), with B more important than A (Cp′ silyl groups have been omitted for clarity). Note that structure B depicts multiple niobium–carbon bond character. Since we know from the studies

(15) Antiñolo, A.; Fajardo, M.; Jalon, F. A.; Lopez Mardomingo, C.; Otero, A.; Sanz-Bernabe, C. *J. Organomet. Chem.* **1989**, *369*, 187–196.

(16) (a) Loehmann, L.; De, R. L.; Trekoval, J. *J. Organomet. Chem.* **1978**, *156*, 307–316. (b) House, H. O.; Auerback, R. A.; Gall, M.; Peet, N. P. *J. Org. Chem.* **1973**, *38*, 514–522.

(17) (a) Manzer, L. E. *Inorg. Chem.* **1977**, *16*, 525–528. (b) Broussier, R.; Normand, H.; Gautheron, B. *J. Organomet. Chem.* **1978**, *155*, 337–346. (c) Al-Mowali, A.; Kuder, W. A. A. *J. Organomet. Chem.* **1980**, *194*, 61–68. (d) Hitchcock, P. B.; Lappert, M. F.; Milne, C. R. C. *J. Chem. Soc., Dalton Trans.* **1981**, 180–186. (e) Bottomley, F.; Keizer, P. N.; White, P. S.; Preston, K. F. *Organometallics* **1990**, *9*, 1916–1925.

(18) (a) Douglas, W. E.; Green, M. L. H. *J. Chem. Soc., Dalton Trans.* **1972**, 1796–1800. (b) Elson, I. H.; Kochi, J. K.; Klabunde, U.; Manzer, L. E.; Parshall, G. W.; Tebbe, F. N. *J. Am. Chem. Soc.* **1974**, *96*, 7374–7376. (c) Elson, I. H.; Kochi, J. K. *J. Am. Chem. Soc.* **1975**, *97*, 1262–1264.

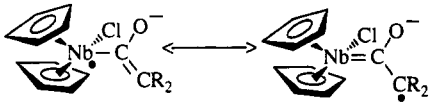

A B

of Lauher and Hoffmann that the available niobium orbitals are contained within the equatorial plane,[19] we can conclude that the metallaenolate must be perpendicular to this plane to support the Nb–C π interaction. We believe that this delocalization is facilitated by the fact that the carbon radical center is *both* tertiary and benzylic.

Voltammetry. We noted earlier that the cyclic voltammograms for the ketene complexes are consistent with an EC mechanism. Since both the first and the second anodic sweeps generate the same wave, we suggest that the new reduction wave is due to a linkage isomer of the starting ketene complex. To see if ketene *E–Z* isomerization was a contributing factor, we also examined $Cp'_2Nb(Cl)(OCCPh_2)$ (**2**), for which an *E–Z* process is unavailable. The voltammogram for **2** (Figure 1b) is clearly similar in shape to that for **1**, and the observation that the corresponding waves for **2** are shifted in the anodic direction relative to those of **1** indicates that there is some ketene character in the frontier orbitals. With both voltammetric and ESR data on the metallaenolates in hand, we propose the cyclic ECEC mechanism enclosed within the dashed lines in Scheme I to explain the voltammetric behavior observed (Figure 1) for the ketene complexes. The sequence begins in the lower left-hand corner with reduction of the ketene complex (**1**) to radical anion ($\mathbf{1}^-$), which then isomerizes to a metallaenolate complex ($\mathbf{4}^-$). Isomerization of $\mathbf{1}^-$ to $\mathbf{4}^-$ is fast; thus a small return wave for the $[Cp'_2Nb(Cl)(ketene)]^{0/-}$ couple can only be seen at higher scan rates (>250 mV/s). This is consistent with a reversible or quasi-reversible $[Cp'_2Nb(Cl)(ketene)]^{0/-}$ couple ($\mathbf{1}/\mathbf{1}^-$) preceding a fast chemical step, as shown in Scheme I. Isomerization of $\mathbf{1}^-$ to $\mathbf{4}^-$ most likely occurs via a twist about the Nb–C bond to produce an enolate ligand which lies perpendicular to the equatorial plane. Thus $\mathbf{4}^-$ corresponds to the canonical structures A and B discussed previously. Upon subsequent oxidation of $\mathbf{4}^-$, an isomer of the initial ketene complex (**4**) is generated; the $[Cp'_2Nb(Cl)(enolate)]^{0/-}$ couple ($\mathbf{4}/\mathbf{4}^-$) is responsible for the reversible electrochemistry seen in the cyclic voltammogram (second sweep) in Figure 1a. We can also surmise that conversion of **4** to **1** is slow since **1** is not present in the second cathodic sweep, even at relatively slow scan rates (e.g., 25 mV/s). However, spectroelectrochemical studies provide evidence that upon oxidation of $\mathbf{4}^-$, **1** is ultimately regenerated (vide infra). Possible formulations for **4** include an *endo*-η^2-C=O-ketene complex,[20] η^1-C-ketene complex,[21] or one of two (*exo* or *endo*)-η^2-C=C-ketene complexes. Although we have been unable to gather sufficient evidence to identify this species unequivocally, we believe the η^1-C-ketene formulation to be the most reasonable. The second voltammetric sweep contained waves which are indicative of a reversible process, and this is inconsistent with a redox-induced structural rearrangement by either species in the redox couple. Since we *have* gathered ESR evidence in favor of the perpendicular metallaenolate anion ($\mathbf{4}^-$), the sequence represented in Scheme I is the most straightforward explanation for the observed data; note that the alternative *endo*-η^2-C=O- or η^2-C=C-ketene complex assignments for **4** would require a geometrical rearrangement in the $\mathbf{4}^-$ → **4** interconversion and would be expected to exhibit behavior similar to that seen in the first sweep (Figure 1). Furthermore, the bonding mode proposed for **4** has been observed in a number of related CO_2 complexes.[21]

Scheme I

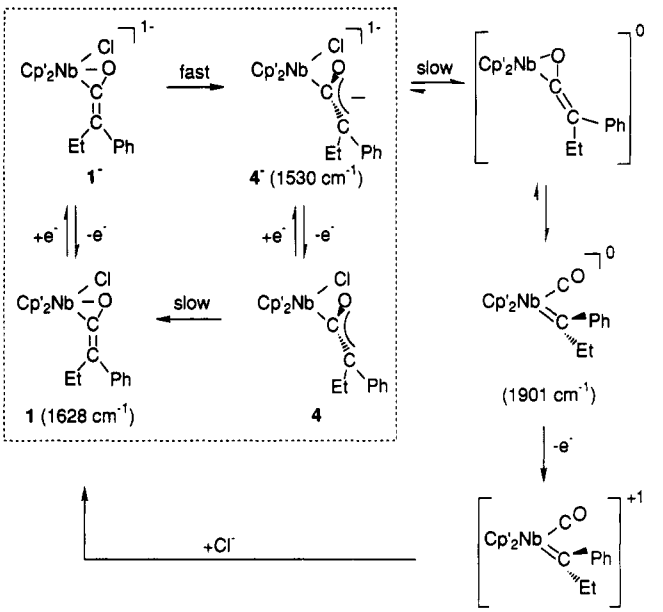

We can also comment on another possible isomerization mechanism. An alternative to the mechanism in Scheme I would involve loss of chloride ligand upon reduction, followed by readdition upon subsequent oxidation. Indeed, a similar mechanism has been postulated for related niobocene halide complexes.[22] However, we disfavor this possibility here for two reasons; first, the addition of chloride has no effect on the voltammetric waves, and second, our spectroelectrochemical data indicate that chloride loss occurs on a time scale greater than that of the voltammetry. Again, the dependence of the peak potentials on the nature of the ketene substituents suggests that this ligand plays an important role in the redox-induced isomerization processes.

Spectroelectrochemical Studies. The mechanism shown in Scheme I is also consistent with the spectral changes observed in the FT-IR spectroelectrochemical studies. In the initial reduction event, ketene complex **1** is converted to metallaenolate complex $\mathbf{4}^-$, which is responsible for the band at 1530 cm^{-1} (Figure 3; the radical ion $\mathbf{1}^-$ is not observed because its isomerization to $\mathbf{4}^-$ is rapid). The metallaenolate is unstable and slowly forms

(19) Lauher, J. W.; Hoffmann, R. *J. Am. Chem. Soc.* **1976**, *98*, 1729–1742.

(20) *endo*-Zirconocene acyls are reported to isomerize to exo isomers: Erker, G.; Rosenfeldt, F. *Angew. Chem., Int. Ed. Engl.* **1978**, *17*, 605–606.

(21) There are several known examples of analogous η^1-C–CO_2 complexes: (a) Gambarotta, S.; Arena, F.; Floriani, C.; Zanazzi, P. F. *J. Am. Chem. Soc.* **1982**, *104*, 5082–5092. (b) Arena, F.; Floriani, C.; Chiesi-Villa, A.; Guastini, C. *Inorg. Chem.* **1986**, *25*, 489–496. (c) Lee, G. R.; Cooper, N. J. *Organometallics* **1985**, *4*, 794–796. (d) Lee, G. R.; Cooper, N. J. *Organometallics* **1985**, *4*, 1467–1468. (e) Jernakoff, P.; Cooper, N. J. *J. Am. Chem. Soc.* **1987**, *109*, 2173–2174. (f) Lee, G. R.; Maher, J. M.; Cooper, N. J. *J. Am. Chem. Soc.* **1987**, *109*, 2956–2962. (g) Guiseppetti, M. E.; Cutler, A. R. *Organometallics* **1987**, *6*, 970–974. (h) Calabrese, J. C.; Herskovitz, T.; Kinney, J. B. *J. Am. Chem. Soc.* **1983**, *105*, 5914–5915. (i) Lundquist, E. G.; Huffman, J. C.; Caulton, K. G. *J. Am. Chem. Soc.* **1986**, *108*, 8309–8310. (j) Giuseppetti-Dery, M. E.; Landrum, B. E.; Shibley, J. L.; Cutler, A. R. *J. Organomet. Chem.* **1989**, *378*, 421–435. (k) Sakaki, S. *J. Am. Chem. Soc.* **1990**, *112*, 7813–7814. (l) Fujita, E.; Creutz, C.; Sutin, N.; Szalda, D. J. *J. Am. Chem. Soc.* **1991**, *113*, 343–353.

(22) (a) Fakhr, A.; Mugnier, Y.; Broussier, R.; Gautheron, B.; Laviron, E. *J. Organomet. Chem.* **1983**, *255*, C8–C10. (b) Naboui, H.; Fakhr, A.; Mugnier, Y.; Antiñolo, A.; Fajardo, M.; Otero, A.; Royo, P. *J. Organomet. Chem.* **1988**, *338*, C17–C20. (c) Naboui, H.; Mugnier, Y.; Fakhr, A.; Laviron, E.; Antiñolo, A.; Jalon, F. A.; Fajardo, M.; Otero, A. *J. Organomet. Chem.* **1989**, *375*, 67–72.

a metal carbonyl complex with a broad band at ca. 1901 cm^{-1} within 10–15 min at room temperature (Figure 4). This process is apparently initiated by chloride loss from 4^-; consistent with this notion, we find that addition of chloride (in the form of (TBA)Cl) inhibits this process in both the spectroelectrochemical and controlled potential electrolysis experiments. We note again that, even in the absence of added chloride, chloride loss from 4^- takes minutes; this verifies that chloride loss cannot contribute to the chemistry observed on the voltammetric time scale. However, partial reduction of 1 to 4^- (2 min at −3.0 V vs SCE) followed immediately by application of a positive potential (2 min at +0.4 V vs SCE) results in the oxidation of 4^- to 1 without appearance of the band at 1901 cm^{-1}.

The loss of chloride from the Nb(IV)–metallaenolate would be expected to give rise to a reduced ketene complex ($Cp'_2Nb(OCCRR')$). Indeed, Antiñolo et al. have presented evidence for a related ketenimine complex $Cp'_2Nb(NPh{=}C{=}CRR')$.[23] While a reduced ketene complex might be responsible for the weak IR band at 1610 cm^{-1}, it constitutes only a small fraction of the species present after chloride loss. The peak at 1901 cm^{-1} is most reasonably attributed to the presence of a metal carbonyl species. Since the potentiostat is off when the niobium(IV) enolate gives way to this compound, and since there is no evidence of enolate disproportionation, the carbonyl is likely a Nb(IV) compound as well. As written in Scheme I, the compound is a 19-electron alkylidene–carbonyl; while this may be an accurate representation, alternate structural possibilities exist. The most likely of these is an isomer with a slipped Cp′, e.g., the 17-electron species (η^5-Cp′)(η^3-Cp′)Nb(=CEtPh)(CO). Unfortunately, Cp slippage is difficult to detect with IR spectroscopy;[24] however, recent studies of associative ligand substitution reactions indicate that the Nb–Cp linkage is indeed prone to slippage.[25] The limited lifetime of the proposed alkylidene precludes isolation; the eventual growth of the IR band at 1920 cm^{-1} is due to the formation of $Cp'_2Nb(Cl)(CO)$,[14] presumably resulting from degradation of the alkylidene compound.

Perhaps the strongest evidence for the formulation of the alkylidene–carbonyl is the observation that some of the starting ketene–chloride complex is regenerated upon oxidation. This (and the IR evidence of a carbonyl ligand) would seem to require the presence of both ketene-derived fragments in the coordination sphere of the metal; this is particularly true of the alkylidene fragment, which would not be stable as a free entity. Upon oxidation, then, the ketene is reformed and the chloride re-enters the coordination sphere. Again, the latter event has a close precedent in the literature. The electrochemistry of various L_2NbCl_2 derivatives (L = Cp, Cp′, and $C_5H_3(SiMe_3)_2$) has been studied by Mugnier and co-workers.[22] They report that reduction generates $[L_2NbCl_2]^-$, which subsequently undergoes loss of chloride to give L_2NbCl or a dimer thereof. The silyl-substituted compound $[(C_5H_4SiMe_3)_2NbCl_2]^-$ undergoes chloride loss more slowly than does $[Cp_2NbCl_2]^-$, presumably because the silyl groups can function as weak π-acceptors which remove the excess charge from the metal center. It has also been observed that subsequent oxidation of the Nb(III) species L_2NbCl is accompanied by reassociation of the chloride to give the starting compound (eq 5).[22c] Our data indicate that chloride loss is even

$$Cp'_2NbCl_2 \xrightarrow{e^-} [Cp'_2NbCl_2]^- \xrightarrow[\text{(slow)}]{-Cl^-} Cp'_2NbCl \qquad (5)$$
$$\uparrow \quad -e^-, +Cl^- \quad \text{(closes the cycle)}$$

slower for the ketene–chloride complex 1, and this is attributed to the fact that the added electron is so efficiently delocalized onto the ketene ligand.

The process described above constitutes a redox-reversible ketene cleavage–formation sequence, and the latter is the route by which ketenes are thought to arise in CO reduction reactions.[6] We noted that this process has been modeled in homogeneous systems, but we are unaware of an example in which it has been redox-induced. In fact, it is interesting that ketene formation is an oxidative process here. Geoffroy and co-workers have utilized trimeric osmium clusters to study the equilibrium between alkylidene–carbonyl and ketene complexes (eq 6), and they

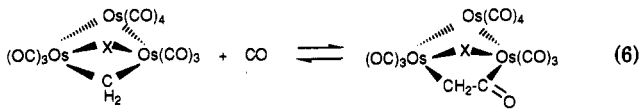

(6)

find that the ancillary ligand X has an important effect.[6e-g] Specifically, electron donors facilitate the formation of ketene ligand, consistent with the acceptor capability of ketene ligands.[26] In the current work, added electron density (via reduction) favors ketene *cleavage* rather than formation. This is not wholly surprising since reduction here also has the effect of opening an adjacent coordination site (via chloride loss); nonetheless, it does provide an interesting comparison with the osmium system.

Two-Electron Chemistry: Electrochemistry in the Presence of Lewis Acid. In contrast to the chemistry discussed above, we observe two-electron processes for bulk electrolyses carried out in an undivided cell with a magnesium counter electrode. Under these conditions, the solution would be expected to contain Mg^{2+} ions which can pair with any niobium–ketene reduction product. There are numerous examples in which coupling a single electron transfer and a proton transfer facilitates a second reduction event.[27] In the current case, a similar scenario could be imagined for the Mg(II) ion. To test for this, we carried out the reaction using a H-cell with a semiporous frit separating the chambers; in this way, we expected to inhibit the interaction of the two electrode products. Indeed, under these circumstances, we observe that the starting ketene complex is depleted in a single electron process (confirmed coulometrically), and an IR spectrum at the end of this reaction showed little or no evidence for the presence of a carbonyl compound. It thus appears that the anode product is required to facilitate the second electron transfer.

We next consider the specific role of the magnesium ion. One possibility is that this Lewis acid aids in the removal of the niobium-bound chloride, while another involves association of the magnesium with the enolate functionality. To differentiate these, we ran the reaction in an undivided cell (magnesium anode) with a 10-fold excess of $NBu_4^+Cl^-$ present; this reagent helped retard the loss of chloride in the one-electron chemistry. In this case, however, it had no deleterious effect on the operation of the two-electron process. We thus favor a mechanism

(23) Antiñolo, A.; Fajardo, M.; Lopez Mardomingo, C.; Otero, A.; Mourad, Y.; Mugnier, Y.; Sanz-Aparicio, J.; Fonseca, I.; Florencio, F. *Organometallics* **1990**, *9*, 2919–2925.
(24) O'Connor, J. M.; Casey, C. P. *Chem. Rev.* **1987**, *87*, 307–318.
(25) Freeman, J. W.; Basolo, F. *Organometallics* **1991**, *10*, 256–263. Also see ref 18c.
(26) Mayr, A.; Asaro, M. F.; Glines, T. J. *J. Am. Chem. Soc.* **1987**, *109*, 2215–2216.
(27) (a) Fry, A. J. *Synthetic Organic Electrochemistry*, 2nd ed.; Wiley-Interscience: New York, 1989; Chapter 4. (b) Peover, M. E. In *Electroanalytical Chemistry*; Bard, A. J., Ed.; Marcel Dekker: New York, 1967; Vol. 2., Chapter 1.

involving a tight association between the metallaenolate and the magnesium, presumably at the enolate oxygen. We have also observed that added Me_3SiCl (used in place of Mg^{2+}) can induce alkyl–carbonyl formation; the obvious similarity between Me_3SiCl and Mg^{2+} is that they both function as oxophilic Lewis acids. The interaction of a Lewis acid with the enolate would help localize excess electron density away from the niobium atom, which would thus resemble a neutral niobium center. This would facilitate a second electron transfer event, presumably resulting in the irreversible loss of the chloride ligand (eq 7). The subsequent chemistry involves addition of a

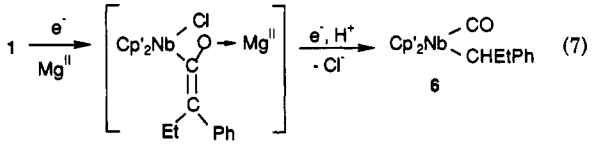

(7)

proton (the origin of which is unclear) and migratory deinsertion to give the alkyl–carbonyl product. Unfortunately, we have been unable to gather evidence regarding the timing of these events, since no intermediates are observed. However, we do believe that the magnesium ion remains in the coordination sphere after the second reduction and that it induces deinsertion at the expense of alternative processes (vide infra). Thus, the key to inducing two-electron chemistry is that the Lewis acid is present while the reducing potential is still being applied.

We have previously reported that the reduction of the ketene–chloride complexes **1–3** in the presence of added ethanol gives rise to the ketene–hydride products $Cp'_2Nb(H)(OCCR_2)$ (**9–11**);[3a] mechanistic evidence suggests that a metallaenolate is protonated by ethanol to give a niobium(IV) acyl, which undergoes a second reduction with loss of chloride and transfer of the acyl β-hydride to the metal (eq 8). This constitutes another example of an acid

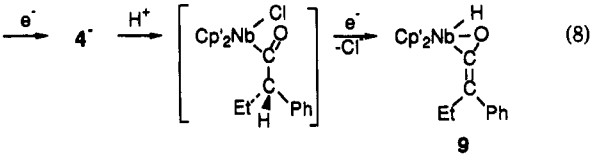

(8)

(a Brønsted acid in this case) coupling with an electron transfer to facilitate a second reduction event and is thus probably related to the magnesium-induced reaction described above. Indeed, if we electrolyze **1** in the presence of excess ethanol (undivided cell, magnesium anode), we observe the ketene–hydride **9** as the sole niobium-containing product; not surprisingly, its formation is accompanied by gas evolution at the cathode (hydrogen from ethanol reduction), but this fails to shut off the two-electron reduction of the niobium compound. This constitutes further support for the notion that the magnesium ion remains bound to the reduction product in eq 7 until it can exert an influence on the migratory deinsertion reaction. Without the magnesium counterion, we would expect to generate the same intermediate (after chloride loss) which leads to β-hydride elimination and ketene–hydride formation.

The difficulty of separating the alkyl–carbonyl from the $Cp'_2Nb(Cl)(CO)$ impurity represents a limitation in the synthetic utility of the process. However, the compounds prepared here contain bulky alkyl ligands that are difficult to introduce via other methodologies. Indeed, α-branched alkyls are often susceptible to isomerization to the *n*-alkyls via a sequence of β-hydride elimination and alkene insertion steps. This can be precluded by the addition of a tightly bound ancillary ligand which blocks the adjacent coordination site needed for elimination (e.g., eq 9).[28] The

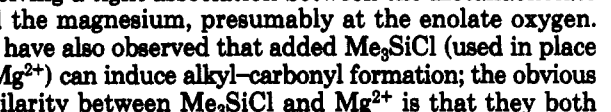

(9)

compounds prepared herein contain an adjacent carbonyl ligand derived from the starting ketene ligand, and we have seen no evidence for isomerization of **6** to the (3-phenylpropyl)niobium isomer.

Regardless of the mechanism involved, the formation of ketene–hydride or alkyl–carbonyl products (using the appropriate conditions for each) is interesting. Both are two-electron processes, and each is coupled with addition of an acid. Moreover, these two compounds are isomeric, exhibiting the same molecular formula and different bonding arrangements. In the hope of establishing a thermodynamic ranking of the two classes of compounds, we have attempted to interconvert the compounds; these efforts involved the addition of a potential ligand to stimulate an insertion process, as well as the addition of catalytic amounts of oxidant to overcome the kinetic inertness often associated with the 18-electron configuration. Thus far we have been unable to effect any interconversion, so it is impossible to identify the thermodynamic isomer. It is known that niobocene alkyl–carbonyls ($Cp_2NbR(CO)$) do not undergo migratory insertion to form acyl compounds, and thermodynamic factors have been implicated.[29] Also known is the fact that other migratory insertions are facilitated by complexation of the carbonyl with a Lewis acid.[30] Thus, it is surprising that (a) it is so easy to observe preferential β-hydride elimination in these reductions and (b) the presence of the Lewis acid is apparently required here to effect a *de*insertion process. We suspect that both of these factors arise from the highly substituted nature of the ligands (acyls or alkyls) derived from the ketenes.

Conclusions. The ketene–chloride complexes exhibit a rich redox chemistry which can be directed along a number of paths. A single-electron process has been observed to give rise to marginally stable compounds identified as alkylidene–carbonyl compounds. Upon reoxidation, these regenerate the ketene ligand; the overall process thus constitutes a redox-induced model for the formation of ketenes from catalytically-relevant precursor ligands. In the presence of acidic substrates, the reductions proceed via two-electron pathways, giving either alkyl–carbonyls (in the presence of Lewis acids) or ketene–hydrides (in the presence of Brønsted acid). All of the chemistry described herein arises from an intermediate paramagnetic metallaenolate, and we have presented coulometric, infrared, and ESR evidence for this species. The latter, in particular, is informative since the small ^{93}Nb hyperfine interaction is highly suggestive of delocalization of the unpaired spin density onto the ligand, a phenomenon which would seem to require a perpendicular disposition of the enolate moiety relative to the equatorial plane. Again, this is wholly

(28) (a) Klazinga, A. H.; Teuben, J. H. *J. Organomet. Chem.* **1980**, *194*, 309–316. (b) Doherty, N. M.; Bercaw, J. E. *J. Am. Chem. Soc.* **1985**, *107*, 2670–2682. (c) Lichtenberger, D. L.; Darsey, G. P.; Kellogg, G. E.; Sanner, R. D.; Young, V. G., Jr.; Clark, J. R. *J. Am. Chem. Soc.* **1989**, *111*, 5019–5028.

(29) (a) Labinger, J. A.; Schwartz, J. *J. Am. Chem. Soc.* **1975**, *97*, 1596–1597. (b) Klazinga, A. H.; Teuben, J. H. *J. Organomet. Chem.* **1979**, *165*, 31–37. (c) Otto, E. E. H.; Brintzinger, H. H. *J. Organomet. Chem.* **1979**, *170*, 209–216. (d) Parshall, G. W.; Schrock, R. R. *Chem. Rev.* **1976**, *76*, 243–268.

(30) (a) Butts, S. G.; Strauss, S. H.; Holt, E. M.; Stimson, R. E.; Alcock, N. W.; Shriver, D. F. *J. Am. Chem. Soc.* **1980**, *102*, 5093–5100. (b) Richmond, T. G.; Basolo, F.; Shriver, D. F. *Inorg. Chem.* **1982**, *21*, 1272–1273. (c) Horowitz, C. P.; Shriver, D. F. *Adv. Organomet. Chem.* **1984**, *23*, 219–305.

consistent with the voltammetric results, which are indicative of a fairly rapid isomerization process concurrent with reduction; spectroelectrochemical studies indicate that this does *not* involve chloride loss, since chloride loss is seen to be a relatively slow process which wouldn't be observed on the voltammetric time scale.

Acknowledgment. ESR analysis software was furnished by the Illinois ESR Research Center, NIH Division of Research Resources Grant No. RR01811. This work was supported by NSF (CHE-9012739 to J.W.B.) and the donors of the Petroleum Research Fund, administered by the American Chemical Society (to M.R.M.B. and A.E.B.). We thank Professors Al Fry and David Westmoreland (Wesleyan University) for helpful discussions and Mr. Tom Jenks (Midac Corp.) for technical assistance.

OM910727J

Synthesis, Characterization, and Reactivity of Triphenylsilyl, Triphenylgermyl, and Triphenylstannyl Derivatives of Zirconium and Hafnium

Hee-Gweon Woo, William P. Freeman, and T. Don Tilley*

Chemistry Department, 0506, University of California at San Diego, 9500 Gilman Drive, La Jolla, California 92093-0506

Received November 8, 1991

The crystalline lithium silyl compound $(THF)_3LiSiPh_3$ (1) was isolated from the reaction of $Ph_3SiSiPh_3$ with lithium in tetrahydrofuran. This compound and tetrahydrofuran solutions of $LiEPh_3$ (E = Ge, Sn) were used to prepare the complexes $CpCp^*Zr(EPh_3)Cl$ (2, E = Si; 3, E = Ge), $CpCp^*Hf(EPh_3)Cl$ (5, E = Si; 6, E = Ge; 7, E = Sn), $Cp^*_2Zr(EPh_3)Cl$ (8, E = Si; 9, E = Ge; 10, E = Sn), and $Cp^*_2Hf(SiPh_3)Cl$ (11). This method did not provide the zirconium stannyl complex $CpCp^*Zr(SnPh_3)Cl$ (4) but instead gave the phenyl derivative $CpCp^*Zr(Ph)Cl$ via phenyl transfer. Compound 4 may be obtained via reactions of $HSnPh_3$ with 2, 3, or $CpCp^*Zr[Si(SiMe_3)_3]Cl$. Reactions of 8 and 11 with MeMgBr gave $Cp^*_2M(SiPh_3)Me$ (12, M = Zr; 13, M = Hf). Hydrogenolysis of 2, 5, 8, and 11 provides routes to the corresponding hydrides $CpCp^*MHCl$ or Cp^*_2MHCl. Likewise, the reactions of 12 and 13 with hydrogen give $Cp^*_2ZrH_2$ and $Cp^*_2Hf(H)Me$, respectively. The germyl and stannyl complexes were found to be significantly less reactive toward hydrogen. Reactions of 2-11 with $PhSiH_3$ gave σ-bond metathesis products in some cases and no reaction in other cases, such that the observed reactivity trends are $CpCp^*M > Cp^*_2M$; Zr > Hf; M-Si > M-Ge > M-Sn. Carbonylation of 8 resulted in formation of $Cp^*_2Zr(\eta^2\text{-}COSiPh_3)Cl$ (14), which reacts with HCl to give the thermally stable formylsilane Ph_3SiCHO (15) and with $2,6\text{-}Me_2C_6H_3NC$ to afford the ketenimine $Cp^*_2Zr[OC(SiPh_3)(CN\text{-}2,6\text{-}Me_2C_6H_3)]Cl$ (16). The silyl complexes 5, 8, and 11 react with $2,6\text{-}Me_2C_6H_3NC$ to give η^2-iminosilaacyl insertion products, as does the germyl 3. However, no reaction is observed between $2,6\text{-}Me_2C_6H_3NC$ and stannyl complexes 7 or 10. These investigations establish the reactivity trends $M\text{-}SiPh_3 > M\text{-}GePh_3 > M\text{-}SnPh_3$ for σ-bond metathesis processes with hydrogen and phenylsilane and for insertion reactions with carbon monoxide and $2,6\text{-}Me_2C_6H_3NC$. It is suggested that, for these analogues d^0 metal silyl, germyl, and stannyl complexes, the energetics of the reactions are influenced primarily by the new E-element bond strengths of the products rather than by the d^0 M-E bond strengths of the starting materials.

Introduction

Investigations of d^0 metal silyl complexes have revealed a number of interesting reactivity patterns that were unprecedented in transition-metal silicon chemistry.[1] This rich reaction chemistry, which involves migratory insertions of unsaturated substrates into metal-silicon bonds[2] and σ-bond metathesis processes which can result in new metal-mediated polymerizations,[3] may be attributed to relatively low d^0 M-Si bond dissociation energies. In light of this, it seemed that analogous d^0 germyl and stannyl complexes, which might possess even weaker M-Ge and M-Sn bonds, would be worth investigating. In addition, comparisons of physical and chemical properties for analogous series of silyl, germyl, and stannyl complexes may be of use in developing a better understanding of bonding interactions in these systems.

Here we report results concerning the synthesis, characterization, and reactivity of analogous $-SiPh_3$, $-GePh_3$, and $-SnPh_3$ complexes of zirconium and hafnium. These

(1) (a) Tilley, T. D. In *The Chemistry of Organic Silicon Compounds*; Patai, S., Rappoport, Z., Eds.; Wiley: New York, 1989; Chapter 24, p 1415 and references therein. (b) Tilley, T. D. In *The Silicon-Heteroatom Bond*; Patai, S., Rappoport, Z., Eds.; Wiley: New York, Chapter 10, p 309.

(2) (a) Campion, B. K.; Heyn, R. H., Tilley, T. D. *Inorg. Chem.* **1990**, *29*, 4355. (b) Woo, H.-G.; Tilley, T. D. *J. Organomet. Chem.* **1990**, *393*, C6. (c) Campion, B. K.; Heyn, R. H.; Tilley, T. D. *J. Am. Chem. Soc.* **1990**, *112*, 2011. (d) Arnold, J.; Engeler, M. P.; Elsner, F. H.; Heyn, R. H.; Tilley, T. D. *Organometallics* **1989**, *8*, 2284. (e) Roddick, D. M.; Heyn, R. H.; Tilley, T. D. *Organometallics* **1989**, *8*, 324. (f) Arnold, J.; Tilley, T. D.; Rheingold, A. L.; Geib, S. J.; Arif, A. M. *J. Am. Chem. Soc.* **1989**, *111*, 149. (g) Elsner, F. H.; Tilley, T. D.; Rheingold, A. L.; Geib, S. J. *J. Organochem. Chem.* **1988**, *358*, 169. (h) Arnold, J.; Tilley, T. D. *J. Am. Chem. Soc.* **1987**, *109*, 3318. (i) Campion, B. K.; Falk, J.; Tilley, T. D. *J. Am. Chem. Soc.* **1987**, *109*, 2049 and references in the above.

(3) (a) Tilley, T. D. *Comments Inorg. Chem.* **1990**, *10*, 37. (b) Harrod, J. F.; Mu, Y.; Samuel, E. *Polyhedron* **1991**, *11*, 1239. (c) Corey, J. In *Advances in Silicon Chemistry*; Larson, G., Ed.; JAI Press, Inc.: Greenwich, CT, 1991; Vol. 1, p 327. (d) Laine, R. M. In *Aspects of Homogeneous Catalysis*; Ugo, R., Ed.; Kluwer Academic Publishers: Amsterdam, 1990; p 37.

0276-7333/92/2311-2198$03.00/0